Homogenization of graphene sheet reinforced composites considering material and geometrical uncertainty

Dimitrios Savvas[1] and †*George Stefanou[2]

[1]Institute of Structural Analysis & Antiseismic Research, National Technical University of Athens, 9 Iroon Polytechneiou, Zografou Campus, 15780 Athens, Greece.
[2]Institute of Structural Analysis & Dynamics of Structures, Department of Civil Engineering, Aristotle University of Thessaloniki, 54124 Thessaloniki, Greece.

*Presenting author: gstefanou@civil.auth.gr
†Corresponding author: gstefanou@civil.auth.gr

Abstract

This paper presents a computational procedure for the determination of the stochastic material properties of defective graphene sheets. The lattice of graphene is modeled using the molecular structural mechanics approach, which is a continuum based nanoscale modeling technique, where the C-C covalent bonds are replaced by energetically equivalent beam elements. The statistical properties for each component of the elasticity matrix are obtained by performing Monte Carlo simulations on randomly generated finite element models of defective graphene sheets. Moreover, computational homogenization of graphene sheet reinforced composites is performed considering material and geometrical uncertainty. The results demonstrate the effect of combined uncertainty on the homogenized properties of the composite material.

Keywords: **Graphene, Vacancy defects, Microstructural uncertainty, Homogenization, Composites.**

Introduction

Graphene is an allotrope of carbon consisting of a single layer of carbon atoms arranged in an hexagonal lattice exhibiting superb mechanical and physical properties (approximately Young's modulus 1 TPa, ultimate strength 130 GPa, thermal conductivity 3000 $W \cdot m^{-1} \cdot K^{-1}$, electric conductivity 2.5×10^5 $cm^2 V^{-1} s^{-1}$). These exceptional properties of graphene along with its high aspect ratio make it ideal reinforcement in composite materials. This is illustrated among others in Aluko et al. [1], where the elastic response of graphene nanoplatelet (GNP) reinforced composites was shown to increase with increased GNP volume fraction, dispersion, and strain rates. Bending and buckling analyses of functionally graded polymer composite plates reinforced with GNP conducted in Song et al. [25] have shown that an addition of a very small amount of GNPs into the polymer matrix can significantly reduce the bending deflections and increase the critical buckling load.

In order to study the mechanical behavior of graphene reinforced polymers, the characterization of the mechanical properties of isolated graphene is important. For this purpose, a lot of experimental [4][11][18] and numerical [16][13][10][24] studies have been conducted. However, there are limited studies computing the mechanical properties of defective graphene lattices (e.g. [2][28][19][20]). A direct experimental evidence for the existence of defects (e.g. topological defects, vacancies and adatoms) in graphene layers has been provided by Hashimoto et al. [5].

In this paper, statistical properties for the components of the elasticity tensor of graphene lattices, which contain randomly dispersed single vacancy defects are computed first. Then, composites containing randomly dispersed graphene sheets to which homogenized stiffness properties have been assigned, are analyzed. The presented numerical results demonstrate the effect of combined material and geometrical uncertainty on the homogenized properties of graphene sheet reinforced composite materials.

Computation of random material properties of graphene sheets

Structure of graphene

Graphene is an allotrope of carbon in the form of a two-dimensional, atomic-scale, hexagonal lattice in which one atom forms each vertex. Each atom has four bonds, one σ-bond with each of its three neighbors and one π-bond that is oriented out of plane. The distance $L_{C\text{-}C}$ between the carbon atoms is about 1.42 Å. Graphene's stability into a single layer of carbon atoms is due to its tightly packed carbon atoms and a sp^2 orbital hybridization. The thickness of a monolayer graphene is about 0.34 nm, which corresponds to the interlayer spacing of graphite and the thickness of one carbon atom.

Graphene is the basic structural element of other allotropes, including graphite and carbon nanotubes which can be formed via stacking and wrapping of the graphene's layers, respectively. Specifically, the helicity of a carbon nanotube is characterized by the roll-up vector $\overrightarrow{C_h}$. This is called the chiral vector and it is defined as:

$$\overrightarrow{C_h} = n\overrightarrow{\alpha_1} + m\overrightarrow{\alpha_2} \tag{1}$$

where $\overrightarrow{\alpha_1} = \left[\sqrt{3}L_{C-C}, 0\right]$ and $\overrightarrow{\alpha_2} = 0.5\left[\sqrt{3}L_{C-C}, 3L_{C-C}\right]$ are basis vectors of length $\sqrt{3}L_{C-C}$ defined on the hexagonal lattice of graphene (see Fig. 1) The pair of indices (n, m) define the chiral angle $\theta_{\overrightarrow{C_h}}$ as

$$\theta_{\overrightarrow{C_h}} = \tan^{-1}\left(\frac{\sqrt{3}m}{2n+m}\right) \tag{2}$$

As it can be deduced from Eq. (2), $\theta_{\overrightarrow{C_h}} = 0°$ for zig-zag direction (m=0) and $\theta_{\overrightarrow{C_h}} = 30°$ for armchair direction (m=n). For all other directions of the chiral vector, $\theta_{\overrightarrow{C_h}} \in (0°, 30°)$.

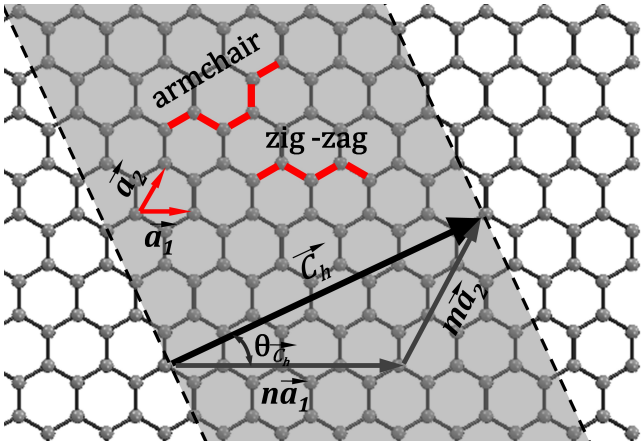

Figure 1. Graphene lattice structure and definition of chiral vector $\overrightarrow{C_h}$.

The molecular structural mechanics approach

The molecular structural mechanics (MSM) approach is a continuum based nanoscale modeling technique developed by Li and Chou [12], which has attracted great attention because of its simplicity and effectiveness. In this framework, the potential energy produced by the C-C atomic interactions is equating to the sum of energies produced by the deformations of a beam element, which substitute the C-C chemical bond. Thus, the method results in a space frame model built by connected beam elements, which is equivalent to the atomistic model of the graphene's lattice. In principle, this approach provides a linkage between molecular mechanics and continuum structural mechanics by which geometry and material properties of the beam elements are obtained.

In the context of molecular mechanics, graphene can be regarded as a molecular system consisting of carbon atoms. The lattice deformation under a specific load is governed by the atomic motions which are regulated by a force field. This force field, which is generated by electron-nucleus and nucleus-nucleus interactions, is usually expressed in the form of a steric potential energy. The general expression of this total steric potential energy is a sum of energies due to valence or bonded and non-bonded interactions as follows:

$$U = U_r + U_\theta + U_\phi + U_\omega + U_{vdW} + U_{es} \tag{3}$$

where U_r, U_θ, U_φ, U_ω are the bond-stretching energy, the bond-angle variation energy, the dihedral-angle torsion energy and the inversion (out of plane torsion) energy, respectively. U_{vdW} and U_{es} are associated with non-bonded van der Waals and electrostatic interactions, respectively, which are usually negligible and therefore are omitted. The corresponding interatomic interactions are schematically represented in Fig. 2.

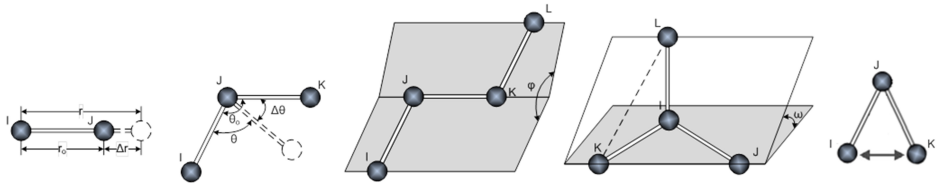

Figure 2. Interatomic interactions in molecular mechanics: a) stretching, b) bending, c) dihedral angle torsion, d) out of plane torsion and e) van der Waals.

By adopting a quadratic potential force field to account for linear covalent C-C interactions and a circular beam element in the context of the finite element (FE) method, the following relationships between structural mechanics parameters and molecular mechanics force field constants are derived

$$d = 4\sqrt{\frac{k_\theta}{k_\tau}},\ E = \frac{k_r^2 L_{C-C}}{4\pi k_\theta},\ G = \frac{k_r^2 k_\tau L_{C-C}}{8\pi k_\theta^2} \tag{4}$$

Substituting the force field constant values k_r=938 kcal·mole^{-1}·Å^{-2}=6.52 x10^{-7} N·nm^{-1}, k_θ=126 kcal·mole^{-1}·rad^{-2}=8.76x10^{-10} N·nm·rad^{-2} and k_τ=40 kcal·mole^{-1}·rad^{-2}=2.78x10^{-10} N·nm·rad^{-2}, defined by Cornell et al. [3], the values of diameter d=0.147 nm, Young's modulus E=5.49 TPa and shear modulus G=0.871 TPa of the beam elements are obtained.

Random material properties of defective graphene sheets

Various structural defects are generated during the production or chemical functionalization process of graphene sheets such as Stone-Wales (SW), single vacancy (SV) and double vacancy (DV) defects [5][14][26]. The most common types of defects are the vacancy defects which are characterized by the number of the absent atoms from the lattice of graphene. In this paper, we will examine graphene sheets containing only SV defects which are formed by removing one carbon atom and its three adjacent bonds from the lattice.

The FE model of a defective graphene sheet is constructed using 2d Bernoulli beams with properties obtained from the MSM approach described in the previous section. The defects are uniformly distributed on the lattice. Each defect is treated as an individual scattering center (independently of the defect type or the number of atoms that forms it). The defect density is defined as $N_d/N_a \times 100$ where N_d and N_a are the number of defects and number of atoms in the pristine graphene, respectively. A FE model of a defective graphene sheet containing 3% randomly dispersed SV defects is shown in Fig. 3.

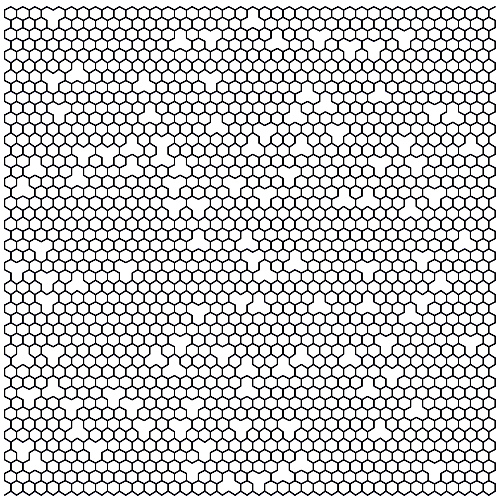

Figure 3. FE model of a defective graphene sheet containing 3% randomly dispersed SV defects.

The homogenized in-plane anisotropic stress-strain relation of the graphene material can be expressed by:

$$\begin{bmatrix} \sigma_1 \\ \sigma_2 \\ \sigma_3 \end{bmatrix} = \begin{bmatrix} C_{11} & C_{12} & C_{13} \\ & C_{22} & C_{23} \\ \text{sym} & & C_{33} \end{bmatrix} \begin{bmatrix} \varepsilon_1 \\ \varepsilon_2 \\ \varepsilon_3 \end{bmatrix} \tag{5}$$

with $[\sigma_1\ \sigma_2\ \sigma_3]^T=[\sigma_{xx}\ \sigma_{yy}\ \sigma_{xy}]^T$ and $[\varepsilon_1\ \varepsilon_2\ \varepsilon_3]^T=[\varepsilon_{xx}\ \varepsilon_{yy}\ \varepsilon_{xy}]^T$ the stress and strain tensors respectively and $\mathbf{C}$ the homogenized anisotropic elasticity tensor. Notice that, due to symmetry, only six components C_{ij}, with i, j=1,2,3 are needed to fully determine the homogenized elasticity matrix. In order to solve for these unknown parameters, three independent uniform strain (Dirichlet) boundary conditions are applied on a square graphene sheet of size 10×10 nm^2, which are derived from the following set of strain deformation cases:

$$\boldsymbol{\varepsilon} = \left\{ \begin{bmatrix} \varepsilon_1 \\ 0 \\ 0 \end{bmatrix}, \begin{bmatrix} 0 \\ \varepsilon_2 \\ 0 \end{bmatrix}, \begin{bmatrix} 0 \\ 0 \\ \varepsilon_3 \end{bmatrix} \right\} \tag{6}$$

Substituting the first strain vector in Eq. (5), the components $C_{11}=\sigma_1/\varepsilon_1$, $C_{21}=\sigma_2/\varepsilon_1$ and $C_{31}=\sigma_3/\varepsilon_1$ can be directly calculated, while the remaining unknown components of **C** are computed in a similar way by applying all other strain vectors of Eq. (6). The statistical properties for each component C_{ij} of the elasticity matrix are obtained by performing 1000 Monte Carlo simulations on randomly generated FE models of defective graphene sheets containing 3% randomly dispersed SV defects. The mean and standard deviation of the average axial stiffness ($C_{ii}/2$, i=1, 2) are calculated as μ=910.73 GPa and σ=29.95 (COV=σ/μ ≈3%), respectively and of the shear stiffness C_{33} as μ=413.63 GPa and σ=16.41 (COV≈4%), respectively. The histograms of $C_{ii}/2$ and C_{33} are depicted in Fig. 4.

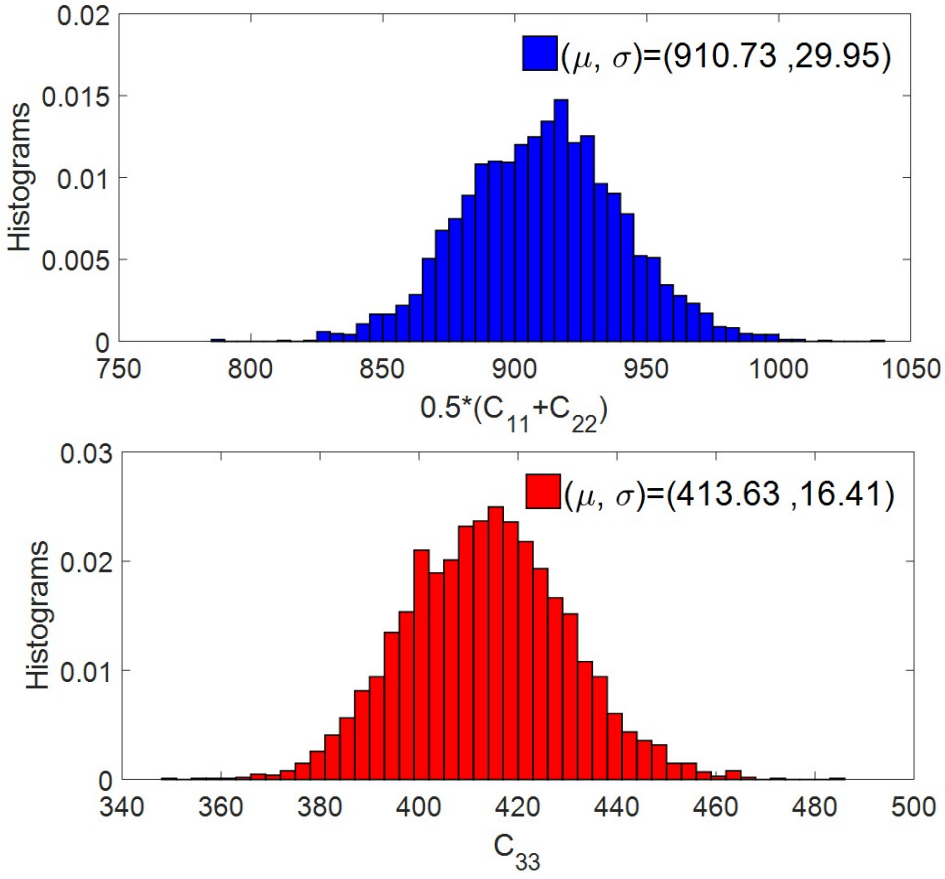

Figure 4. Histograms for average axial stiffness and shear stiffness of graphene sheet with 3% randomly dispersed SV defects obtained from 1000 Monte Carlo simulations.

Determination of effective material properties for graphene sheet reinforced composites

The computational procedure for the determination of effective material properties for graphene sheet reinforced composites is illustrated in Fig. 5. In the first step, 1000 Monte Carlo simulations are performed in order to compute the statistical properties for the components of the elasticity tensor of defective graphene lattices containing 3% randomly dispersed SV defects. The graphene lattices are analyzed using the MSM approach described previously. Then, homogenized graphene sheets with material properties considered as

random variables are randomly dispersed into a polymer matrix. The resulting composites are analyzed using the extended finite element method (see Savvas et al. [23]) and homogenized mechanical properties are computed by performing Monte Carlo simulations as described in the next section.

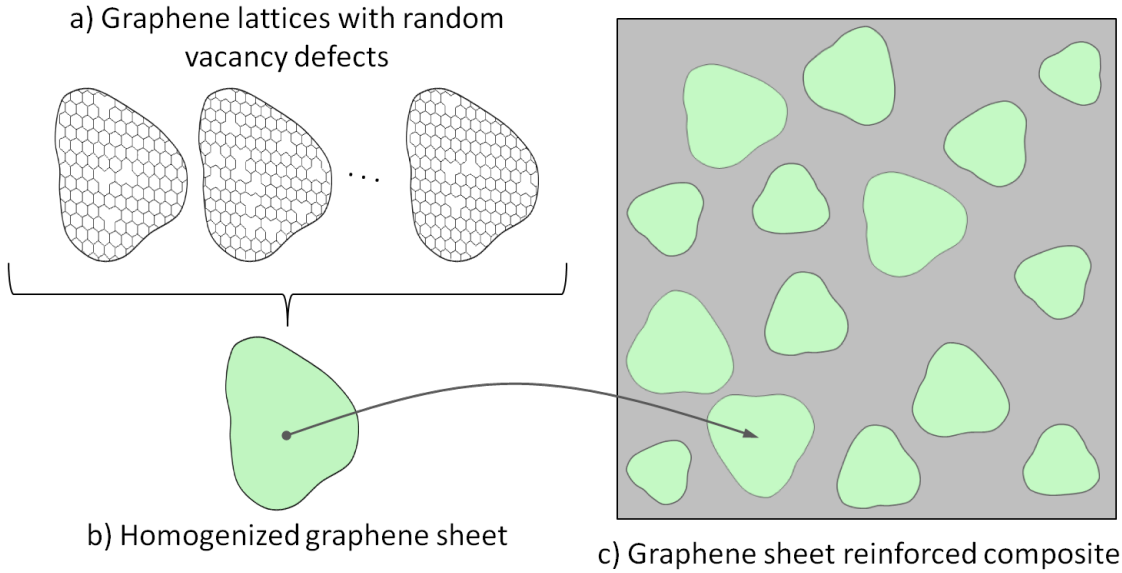

Figure 5. a) Graphene lattices with random vacancy defects, b) Homogenized graphene sheet derived from Monte Carlo simulation and homogenization, c) Graphene sheet reinforced composite material with random dispersion of inclusions.

Computational homogenization

The homogenization scheme adopted in this paper is based on the fundamental assumption of statistical homogeneity of the heterogeneous medium [6] which means that all statistical properties of the state variables are the same at any material point and thus a representative volume element (RVE) can be identified. It has been shown in the literature that the size of the RVE is related to a scale factor $\delta=l_{meso}/l_{micro}$ (under the condition $l_{micro}<<l_{meso}$ with l_{micro} the length scale of the reinforcement (e.g. diameter, thickness, length) and l_{meso} the length scale of the examined volume element [17] [27][21][22]. Satisfaction of this condition leads to homogenized material properties independent of the type of the boundary conditions imposed on the model. Note also that the relation $l_{meso}<< l_{macro}$, with l_{macro} denoting the characteristic length over which the macroscopic loading varies in space, must always hold for complete separation of scales. In this case, the uniformity of microscopic stress and strain fields near the boundary surface $\partial\Omega$ of the mesoscale model Ω, required in the context of Hill's homogenization theory, is valid [8].

The Hill-Mandel homogeneity condition postulates that the strain energy computed on a material point of the macro-continuum medium has to be equal to that computed over the mesoscale volume element in an average sense:

$$\bar{\boldsymbol{\sigma}} : \bar{\boldsymbol{\varepsilon}} = \frac{1}{|V|}\int_{\Omega} (\boldsymbol{\sigma} : \boldsymbol{\varepsilon})\, dx \tag{7}$$

where V is the volume of the mesoscale volume element and the macroscopic stresses and strains are computed as:

$$\bar{\boldsymbol{\sigma}} = \frac{1}{|V|}\int_{\Omega}\boldsymbol{\sigma}(x)dx,\ \bar{\boldsymbol{\varepsilon}} = \frac{1}{|V|}\int_{\Omega}\boldsymbol{\varepsilon}(x)dx \tag{8}$$

Eq. (8) is valid provided that the following constraint is satisfied:

$$\frac{1}{|V|}\int_{\partial\Omega}(t-\bar{\boldsymbol{\sigma}}\cdot n)(u-\bar{\boldsymbol{\varepsilon}}\cdot x)dS = 0 \tag{9}$$

which is a priori satisfied by both kinematic uniform boundary conditions (KUBCs) and static uniform boundary conditions (SUBCs) as shown in Huet [9]. The constraint of Eq. (9) can be also satisfied by orthogonal uniform mixed boundary conditions (OUMBCs) [7] and periodic boundary conditions (PBCs) [15].

Miehe and Koch [15] proposed a computational procedure to define homogenized stresses and overall tangent moduli of microstructures undergoing small strains. They have shown that homogenized properties can be defined in terms of discrete forces and stiffness properties on the boundary of discretized microstructures. Using these deformation-driven algorithms, the homogenized elasticity tensor of a mesoscale model can be calculated by solving a kinematic uniform or a static uniform boundary value problem.

Specifically, for the case of kinematic uniform boundary conditions, a prescribed uniform strain tensor $\bar{\boldsymbol{\varepsilon}} = \left[\bar{\varepsilon}_{11},\ \bar{\varepsilon}_{22},\ 2\bar{\varepsilon}_{12}\right]$ is applied on the boundary $\partial\Omega$ of a discretized mesoscale model Ω through displacements in the form:

$$u_b = \mathbf{D}_b^{\mathbf{T}}\bar{\boldsymbol{\varepsilon}} \tag{10}$$

where $\mathbf{D_b}$ is a geometric matrix which depends on the coordinates of the boundary node b and is defined as:

$$\mathbf{D_b} = \frac{1}{2}\begin{bmatrix} 2x_b & 0 \\ 0 & 2y_b \\ y_b & x_b \end{bmatrix} \text{ with } (x_b,\ y_b) \in \partial\Omega \tag{11}$$

Note that the stiffness matrix $\mathbf{K}$ of the extended finite element model of the graphene sheet reinforced composite can be rearranged into sub-matrices associated with interior nodes i and boundary nodes b. Thus the static problem is denoted by:

$$\begin{bmatrix} K_{ii} & K_{ib} \\ K_{bi} & K_{bb} \end{bmatrix}\begin{bmatrix} U_i \\ U_b \end{bmatrix} = \begin{bmatrix} F_i \\ F_b \end{bmatrix} \tag{12}$$

Then the homogenized elasticity tensor $\mathbf{C}(\theta)$ can be calculated in terms of the condensed stiffness matrix $\tilde{K}_{bb} = K_{bb} - K_{bi}K_{ii}^{-1}K_{ib}$ in the form:

$$\mathbf{C}(\theta) = \frac{1}{|V|}\mathbf{D}\tilde{K}_{bb}\mathbf{D}^{T} \tag{13}$$

where $\mathbf{D} = \left[D_1\ D_2 \cdots D_M\right]$ with M the total number of boundary nodes. Note that θ denotes the randomness of the computed homogenized elasticity tensor due to material uncertainty related to the random properties assigned to graphene sheets and to geometrical uncertainty related to the random dispersion of the inclusions (graphene sheets) within the composite material.

Numerical results

In this section, the two sources of microstructural uncertainty (material and geometrical) are considered simultaneously and their effect on the homogenized constitutive properties of the composite material is assessed. Note that the composites are assumed to be under plane stress conditions. The statistical properties of the homogenized material for the graphene sheets have been calculated in a previous section. The material of the matrix is considered isotropic and linearly elastic with Young's modulus E_m=1 GPa and Poisson's ratio v_m=0.3. Fig. 6 illustrates the empirical distribution and the statistical convergence of mean and COV of the axial stiffness $C_{ii}/2$ (i=1,2) of the graphene sheet reinforced composite material. Similar results are presented in Fig. 7 for the shear stiffness C_{33}. Note that all composites are reinforced with 40% vf of graphene sheets with arbitrary shape (see Fig. 5). It is noted that the first two statistical moments of the average axial and shear stiffness of the above composites seem to converge sufficiently within 1000 Monte Carlo simulations.

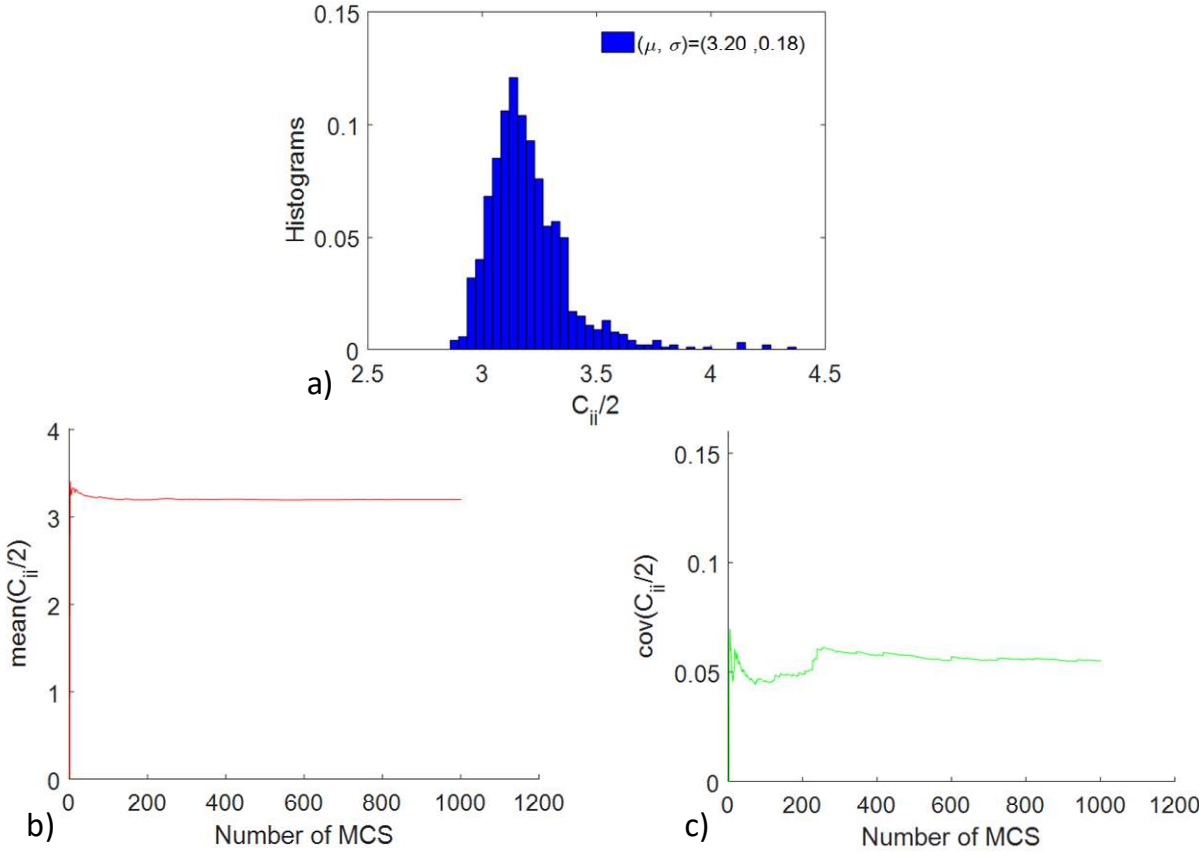

Figure 6. a) Histogram of average axial stiffness $C_{ii}/2$, b) Statistical convergence of mean($C_{ii}/2$) with respect to the number of Monte Carlo simulations, c) Statistical convergence of COV($C_{ii}/2$) with respect to the number of Monte Carlo simulations.

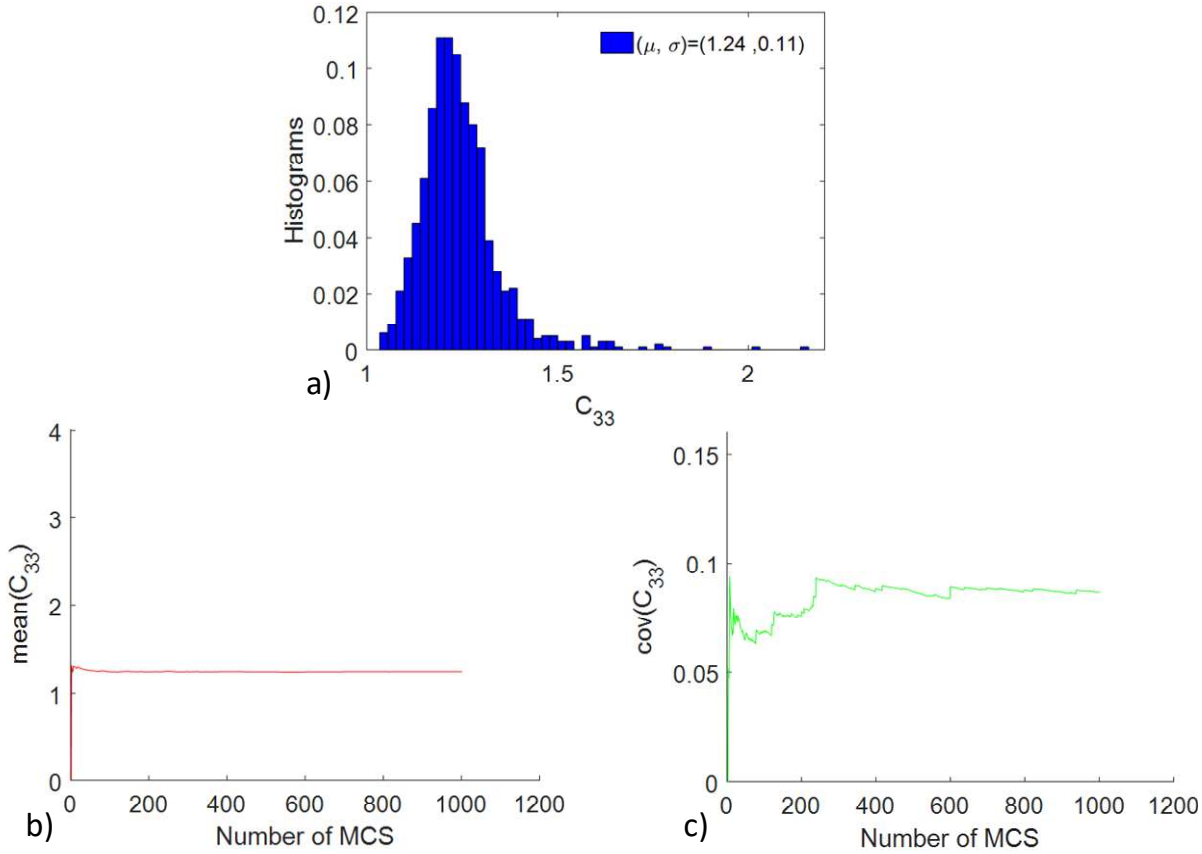

Figure 7. a) Histogram of shear stiffness C_{33}, b) Statistical convergence of mean(C_{33}) with respect to the number of Monte Carlo simulations, c) Statistical convergence of COV(C_{33}) with respect to the number of Monte Carlo simulations.

Conclusions

In this paper, the effect of the two sources of microstructural uncertainty (material and geometrical) on the homogenized elastic properties of graphene sheet reinforced composites was assessed. The lattice of graphene was modeled using the molecular structural mechanics approach. The statistical properties for each component of the elasticity matrix were obtained by performing Monte Carlo simulations on randomly generated finite element models of defective graphene sheets. Subsequently, computational homogenization of graphene sheet reinforced composites was performed considering material and geometrical uncertainty. A magnification of uncertainty was observed, as the COV of the material properties of the composite was larger than the corresponding COV of the reinforcements, especially in the case of shear stiffness.

References

[1] Aluko, O., Gowtham, S., and Odegard, G. (2017). Multiscale modeling and analysis of graphene nanoplatelet/carbon fiber/epoxy hybrid composite. *Composites Part B: Engineering*, **131**:82-90.

[2] Askari, D. and Ghasemi-Nejhad, M. N. (2011). Effects of vacancy defects on mechanical properties of graphene/carbon nanotubes: A numerical modeling. *Journal of Computational and Theoretical Nanoscience*, **8**(4):783-794.

[3] Cornell, W. D., Cieplak, P., Bayly, C. I., Gould, I. R., Merz, K. M., Ferguson, D. M., Spellmeyer, D. C., Fox, T., Caldwell, J. W., and Kollman, P. A. (1995). A second generation force field for the simulation of proteins, nucleic acids, and organic molecules. *Journal of the American Chemical Society*, **117**(19):5179-5197.

[4] Frank, I., Tanenbaum, D. M., van der Zande, A. M., and McEuen, P. L. (2007). Mechanical properties of suspended graphene sheets. *Journal of Vacuum Science & Technology B: Microelectronics and Nanometer Structures Processing, Measurement, and Phenomena*, **25**(6):2558-2561.

[5] Hashimoto, A., Suenaga, K., Gloter, A., Urita, K., and Iijima, S. (2004). Direct evidence for atomic defects in graphene layers. *Nature*, **430**(7002):870.
[6] Hashin, Z. (1983). Analysis of composite materials: A survey. *Journal of Applied Mechanics*, **50**(2):481-505.
[7] Hazanov, S. and Huet, C. (1994). Order relationships for boundary conditions effect in heterogeneous bodies smaller than the representative volume. *Journal of the Mechanics and Physics of Solids*, **42**(12):1995-2011.
[8] Hill, R. (1963). Elastic properties of reinforced solids: some theoretical principles. *Journal of the Mechanics and Physics of Solids*, **11**(5):357-372.
[9] Huet, C. (1990). Application of variational concepts to size effects in elastic heterogeneous bodies. *Journal of the Mechanics and Physics of Solids*, **38**(6):813-841.
[10] Jiang, J.-W., Wang, J.-S., and Li, B. (2009). Young's modulus of graphene: A molecular dynamics study. *Physical Review B*, **80**:113405.
[11] Lee, C., Wei, X., Kysar, J. W., and Hone, J. (2008). Measurement of the elastic properties and intrinsic strength of monolayer graphene. *Science*, **321**(5887):385-388.
[12] Li, C. and Chou, T.-W. (2003). A structural mechanics approach for the analysis of carbon nanotubes. *International Journal of Solids and Structures*, **40**(10):2487-2499.
[13] Liu, F., Ming, P., and Li, J. (2007). Ab initio calculation of ideal strength and phonon instability of graphene under tension. *Physical Review B*, **76**(6):064120.
[14] Liu, L., Qing, M., Wang, Y., and Chen, S. (2015). Defects in graphene: generation, healing, and their effects on the properties of graphene: a review. *Journal of Materials Science & Technology*, **31**(6):599-606.
[15] Miehe, C. and Koch, A. (2002). Computational micro-to-macro transitions of discretized microstructures undergoing small strains. *Archive of Applied Mechanics*, **72**(4-5):300-317.
[16] Odegard, G. M., Gates, T. S., Nicholson, L. M., and Wise, K. E. (2002). Equivalent-continuum modeling of nano-structured materials. *Composites Science and Technology*, **62**(14):1869-1880.
[17] Ostoja-Starzewski, M. (2006). Material spatial randomness: From statistical to representative volume element. *Probabilistic engineering mechanics*, **21**(2):112-132.
[18] Poot, M. and van der Zant, H. S. (2008). Nanomechanical properties of few-layer graphene membranes. *Applied Physics Letters*, **92**(6):063111.
[19] Rafiee, R. and Eskandariyun, A. (2017). Comparative study on predicting young's modulus of graphene sheets using nano-scale continuum mechanics approach. *Physica E: Low-dimensional Systems and Nanostructures*, **90**:42-48.
[20] Savvas, D. and Stefanou, G. (2018). Determination of random material properties of graphene sheets with different types of defects. *Composites Part B: Engineering*, **143**:47-54.
[21] Savvas, D., Stefanou, G., Papadopoulos, V., and Papadrakakis, M. (2016a). Effect of waviness and orientation of carbon nanotubes on random apparent material properties and rve size of cnt reinforced composites. *Composite Structures*, **152**:870-882.
[22] Savvas, D., Stefanou, G., and Papadrakakis, M. (2016b). Determination of rve size for random composites with local volume fraction variation. *Computer Methods in Applied Mechanics and Engineering*, **305**:340-358.
[23] Savvas, D., Stefanou, G., Papadrakakis, M., and Deodatis, G. (2014). Homogenization of random heterogeneous media with inclusions of arbitrary shape modeled by XFEM. *Computational Mechanics*, **54**(5):1221-1235.
[24] Shokrieh, M. M. and Rafiee, R. (2010). Prediction of Young's modulus of graphene sheets and carbon nanotubes using nanoscale continuum mechanics approach. *Materials & Design*, **31**(2):790-795.
[25] Song, M., Yang, J., and Kitipornchai, S. (2018). Bending and buckling analyses of functionally graded polymer composite plates reinforced with graphene nanoplatelets. *Composites Part B: Engineering*, **134**:106-113.
[26] Tian, W., Li, W., Yu, W., and Liu, X. (2017). A review on lattice defects in graphene: Types, generation, effects and regulation. *Micromachines*, **8**(5):163.
[27] Trovalusci, P., Ostoja-Starzewski, M., De Bellis, M. L., & Murrali, A. (2015). Scale-dependent homogenization of random composites as micropolar continua. *European Journal of Mechanics-A/Solids*, **49**, 396-407.
[28] Tserpes, K. I. (2012). Strength of graphenes containing randomly dispersed vacancies. *Acta Mechanica*, **223**(4):669-678.